Journal of
Synchrotron
Radiation

ISSN 0909-0495

Received 1 October 2009
Accepted 24 January 2010

Application of magnetic Compton scattering for spin-specific magnetic hysteresis measurement

Akane Agui,[a]* Hiroshi Sakurai,[b] Takuro Tamura,[b] Toshitaka Kurachi,[b] Masahito Tanaka,[c] Hiromichi Adachi[d] and Hiroshi Kawata[d]

[a]Synchrotron Radiation Research Center, Japan Atomic Energy Agency, 1-1-1 Kouto, Sayo-cho, Sayo-gun, Hyogo 679-5148, Japan, [b]Department of Electronic Engineering, Gunma University, 1-5-1 Tenjin-cho, Kiryu, Gunma 376-8515, Japan, [c]National Institute of Advanced Industrial Science and Technology (AIST), 1-1-1 Umezono, Tsukuba, Ibaraki 305-8561, Japan, and [d]Photon Factory, Institute of Materials Structure Science, High Energy Accelerator Research Organization, 1-1 Oho, Tsukuba, Ibaraki 305-0801, Japan. E-mail: agui@spring8.or.jp

An application of magnetic Compton scattering as a new tool to measure a spin-specific magnetic hysteresis (SSMH) loop is introduced and its validity demonstrated. The applied magnetic field dependence of the integrated intensity of magnetic Compton scattering spectra, which reflect only the spin-dependent magnetic properties of magnetically active electrons, was interpreted as the spin-specific hysteresis. The spin magnetization of amorphous $Tb_{33}Co_{67}$ film was observed and its SSMH loop exhibited qualitative agreement with the ordinal magnetic hysteresis loop measured using a conventional vibrating sample magnetometer.

Keywords: Compton scattering; spin moment; amorphous film; thin film; hysteresis loop; TbCo; magnetization.

1. Introduction

Compton scattering has been well known as a quantum property of photons since it was first reported in the 1920s (Cooper *et al.*, 2004). Its profile corresponds to the double-integral of electron momentum. In the 1970s, specific use of magnetic Compton scattering for the study of magnetism was proposed. Later, since the 1980s, highly brilliant circularly polarized X-rays have been produced at synchrotron radiation facilities, thus promoting the study of magnetic materials using magnetic Compton scattering (Sakai & Oono, 1976). Since the short wavelength of the incident X-rays allows impulse approximation, magnetic Compton scattering intensity reflects only the spin magnetic moment component of a magnetically active electron (Sakai, 1996). This is a great advantage when investigating microscopic magnetic properties of materials, in particular spin-specific innate properties; Compton scattering measurements have a unique advantage in that the spin magnetic moment of magnetic electrons in condensed matter can be directly studied. For example, magnetic Compton scattering measurements have been used to show that the magnetic anisotropy of rare-earth (RE) transition metal (TM) amorphous film is induced by the asymmetry of the wave-function of magnetic electrons (Liu *et al.*, 2007; Sakurai *et al.*, 2007).

Properties of magnetic materials are determined in most situations by measuring their magnetization as a function of an external magnetic field. Most cases of magnetic hysteresis are measured with a probe which detects the macroscopic magnetic properties of the sample, for example by using a vibrating-sample magnetometer (VSM). In a way, macroscopic magnetic properties are based on microscopic magnetic characteristics, *e.g.* the magnetic moment of magnetically active elements of a sample. For study of microscopic magnetic properties, Chen *et al.* (1993) first demonstrated the feasibility of element-specific magnetic hysteresis (ESMH) measurement by using magnetic circular dichroism (MCD) measurement with circularly polarized synchrotron radiation. ESMH consists of both orbital moment and spin moment properties, and these probably cannot be separated.

The spin-dependent Compton scattering cross section to find a final photon in a fixed direction with an energy between ω_2 and $\omega_2 + \mathrm{d}\omega_2$ in the solid angle of scattered photons $\mathrm{d}\Omega$ in Plank units is

$$\begin{aligned}\mathrm{d}^2\sigma/\mathrm{d}\Omega\,\mathrm{d}\omega_2 = {} & \left(e^4/16m^2\right)(\omega_2/\omega_1) \\ & \times\big[\left(1+\cos^2\theta\right)+\sin^2\theta P_{1\mathrm{L}} \\ & +(1/m)P_{1\mathrm{C}}(\cos\theta-1)\times\boldsymbol{\sigma}\cdot(\mathbf{k}_1\cos\theta+\mathbf{k}_2)\big] \\ & \times J\left(\sigma,p_z\right).\end{aligned} \quad (1)$$

Here, the symbol m is the electron rest mass, e is the electron charge including its sign, p is the momentum of the electron and $\boldsymbol{\sigma}$ are Pauli matrices. Also, the symbols $\mathbf{k}_1$ and $\mathbf{k}_2$ are the wavevectors for the incident and scattered X-rays, respectively, and ω_1 and ω_2 are the energies of the incident and scattered X-rays, respectively. The symbol θ is the angle between the wavevectors $\mathbf{k}_1$ and $\mathbf{k}_2$. P_{1L} and P_{1C} are the Stokes parameters for linear and circular polarization, respectively. The z axis is defined to be parallel to $\mathbf{k}_1$. The quantity $J(\sigma, p_z)$ is the spin-up or spin-down Compton profile. If a sample is magnetized in the direction parallel to the vector $\mathbf{k}_1 \cos\theta + \mathbf{k}_2$, we can obtain the spin projection of the sample magnetization. The spin-dependent Compton scattering cross section changes its sign when the spin direction is reversed or the helicity of the circular polarization changes (Sakai, 1996). We can assume that the intensity difference between spin-up and spin-down Compton profiles is the magnetic effect of Compton scattering and consider that it is proportional to $J(\sigma, p_z)$.

In this study, we utilized the dependence of the intensity of the magnetic Compton profile, *i.e.* the magnetic effect of Compton scattering, of a thin film of amorphous TbCo on the applied magnetic field to obtain information on spin magnetization, in other words the spin-specific magnetic hysteresis (SSMH) loop. The obtained microscopic hysteresis loop was compared with the macroscopic hysteresis loop which was measured using a conventional VSM.

2. Experimental and experimental procedure

A sample of a $Tb_{33}Co_{67}$ amorphous film was fabricated by the DC sputtering method. The thickness of the $Tb_{33}Co_{67}$ film was 1 µm, and the film was grown on Kapton film with a thickness of 12.8 µm.

The macroscopic magnetization curve of the $Tb_{33}Co_{67}$ film at room temperature was measured perpendicular to the film surface using a conventional VSM.

The magnetic Compton profile (MCP) measurements were carried out at the AR-NE1A1 beamline (Kawata *et al.*, 1989) of KEK-PF (High Energy Accelerator Research Organization, Institute of Materials Structure Science, Photon Factory) in Tsukuba, Japan. Fixed circularly polarized X-rays from an elliptical multipole wiggler (EMPW) were used as incident beam. While the ring was operating at 6.5 GeV and 50 mA, a typical beam lifetime was 16 h. The degree of circular polarization was about 0.66. The energy of the monochromated X-rays was set to be 50 keV in order to avoid fluorescence ($K\alpha$ and $K\beta$ from Tb) and thus obtain good quality magnetic Compton scattering signals. The incident X-ray beam size was about 0.5 mm × 0.5 mm at the sample position. The intensity of the incident beam was monitored using an Ar gas ionization chamber. The incident X-rays were tilted 10° away from the applied field direction. Compton-scattered X-rays were detected over a scattering angle of 160° by a six-segmented Ge solid-state detector (Sakai *et al.*, 1991). The sample was set in a superconducting magnet which was able to apply a magnetic field between −2 T and 2 T. The field was applied in the direction normal to the sample surface. The MCPs were measured by reversing the magnetic field of the superconducting magnet at room temperature. Since an EMPW is commonly used to provide fixed polarized X-rays, a superconducting magnet was used in order to change the direction of magnetization of the sample. In order to achieve a higher signal-to-noise ratio, we prepared the specimen by laying 27 sheets of the film one on top of another. The experimental set-up is illustrated on the left-hand side of Fig. 1.

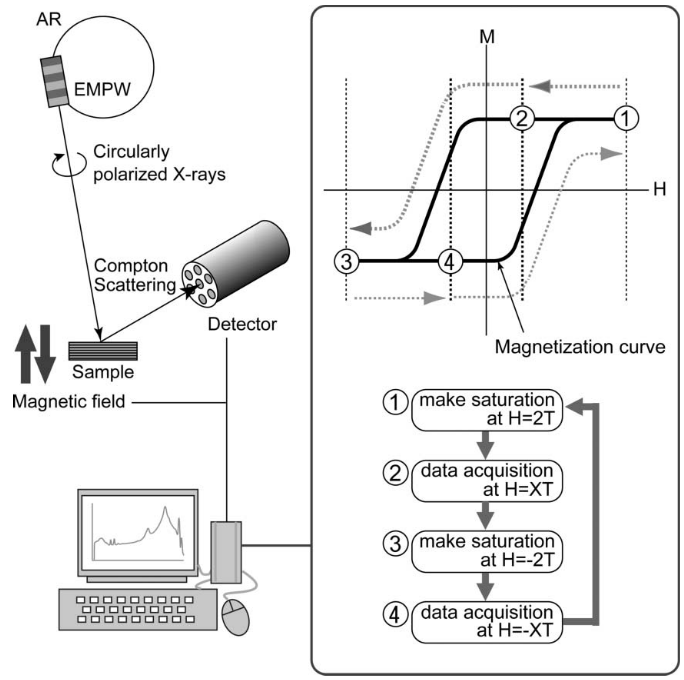

Figure 1
Illustration of the experimental set-up and procedure for measurement of the applied magnetic field dependence of the integrated intensity of the magnetic Compton scattering to obtain the spin magnetization curve.

A set of two spectra, I^+ and I^-, were measured alternately and repeatedly, where I denotes the integrated intensity of Compton scattering. The superscript + (−) indicates that the sample magnetization is parallel (anti-parallel) to the polarized X-rays. By taking the difference between I^+ and I^- we obtain the spin-dependent Compton scattering component only. The procedure to measure SSMH is shown on the right-hand side of Fig. 1. The sequence was controlled by a computer program. For example, to measure the magnetic effect at $H = X$ T, the highest magnetic field (1; $H = 2$ T) was first applied to saturate the sample and then the target field (2; $H = X$ T) was applied for measurement, and, further, the lowest magnetic field (3; $H = -2$ T) was applied to saturate the sample and then the target field (4; $H = -X$ T) was applied for measurement. Then, the effect of the MCP at $H = X$ T was obtained by $(I^+ - I^-)/(I^+ + I^-)$ when X was a positive value. When X was a negative value, the effect of the MCP was obtained by $(I^- - I^+)/(I^+ + I^-)$. The data acquisition time was typically 60 s and the process was repeated typically 120 times.

3. Results and discussion

Fig. 2 shows the MCP of $Tb_{33}Co_{67}$ measured at (*a*) $H = 2$ T and (*b*) $H = 0.2$ T. The dots and the solid line show the measurement result and a curve-fitting result for the MCP, respectively. The fitted line is a linear combination of the Tb 4f Compton profile (Biggs *et al.*, 1975) and the Co 3d Compton profile (Kakutani *et al.*, 2003). The region under 1.5 a.u. in the MCP

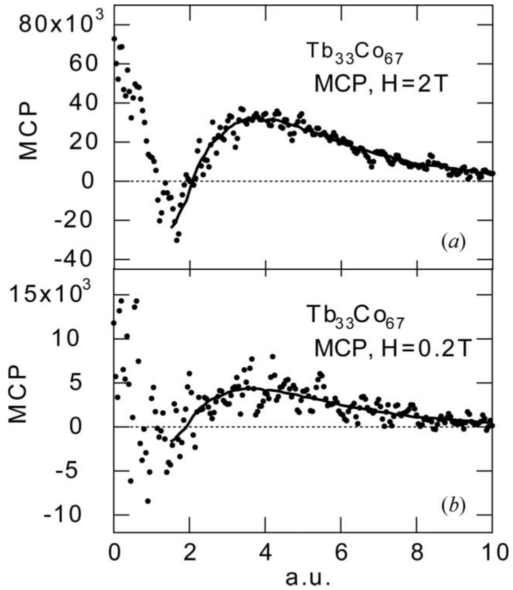

Figure 2
Magnetic Compton scattering profiles of amorphous $Tb_{33}Co_{67}$ film in applied magnetic fields of (*a*) H = 2 T and (*b*) H = 0.2 T. Solid curves are curve-fitting results.

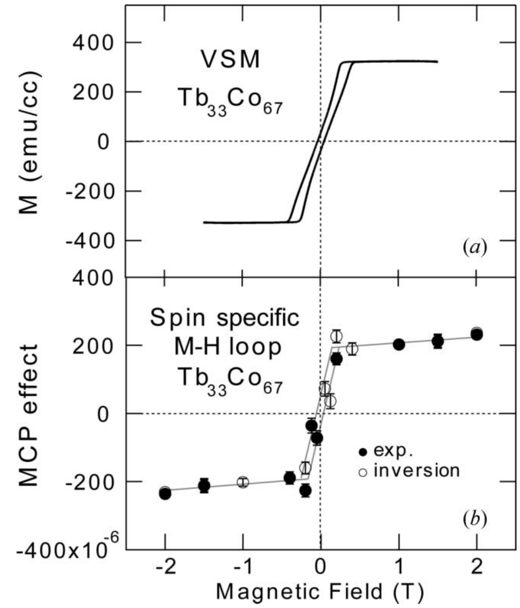

Figure 3
(*a*) The *M*–*H* hysteresis loop of amorphous $Tb_{33}Co_{67}$ in the direction perpendicular to the film surface measured by VSM. (*b*) Spin magnetization curve of $Tb_{33}Co_{67}$ amorphous film, *i.e.* the SSMH loop, obtained by magnetic Compton scattering measurement. Closed circles show the direct result of measurement and open circles are their inversion. The grey lines are guides for the eyes.

is neglected, in which the MCP is dominated by itinerant components, to obtain the fitted line because the curve-fitting processes were treated within a local moment assumption. The fitting results show that the contributions from Tb 4*f* and Co 3*d* components are in opposite magnetic directions in the film, and the ratio is ~6:5. Our previous MCD measurements have shown that the magnetic moment of Tb 4*f* and Co 3*d* are oppositely oriented (Agui *et al.*, 2004, 2007) owing to sperri magnetic structure (Coey, 1978). The present results show that even in the case of spin moment alone the Tb 4*f* and Co 3*d* moments are oppositely oriented. The good fitting result implies that the spin magnetic moment in $Tb_{33}Co_{67}$ film consists of a Tb 4*f* spin magnetic moment and a Co 3*d* spin magnetic moment.

Fig. 3(*a*) shows the macroscopic magnetic hysteresis loops of one sheet of $Tb_{33}Co_{67}$ film measured with a VSM. It shows that the magnetization of the film is saturated over H = 0.45 T and the magnetic coercivity (H_c) is 0.04 T.

Fig. 3(*b*) shows the effect of the MCP with error bars, as a function of the applied magnetic field. Because this measurement is time-consuming owing to the low magnetic effect of the sample, we only measured a limited number of points, forming only about half of the hysteresis loop. The inversion of the measured points was calculated to form the other half of the loop. Closed circles show the direct result of measurement and open circles are their inversion. The grey lines are guides for the eyes. In this way we successfully obtained the SSHM loop.

Figs. 3(*a*) and 3(*b*) show a macroscopic *M*–*H* hysteresis loop, measured using a VSM, and the present microscopic SSMH loop, respectively; both show a qualitatively similar behaviour. The effect of the MCP is almost zero at H = 0.04 T (also at H = −0.04 T). This magnetic field corresponds to H_c measured by the VSM. This implies that the microscopic spin magnetic moment vanishes owing to the sum of the Tb 4*f* and Co 3*d* spin moment becoming zero. Furthermore, Fig. 3(*b*) shows that the hysteresis loop closes at about $H > 0.44$ T. In this study we used stacked TbCo film as the test specimen, and it was expected that local effects, such as domain states, would then be averaged. Moreover, since the Compton scattering measurement was carried out using hard X-ray beams, which have a large penetration depth, the MCP extracts spin information from the entire specimen, not only information on the surface state. Thus, these facts allow comparison of the SSMH hysteresis loop with the VSM *M*–*H* hysteresis loop. Our previous MCD measurements have found that the macroscopic magnetism of RE-TM amorphous film is dominated by the orbital magnetic moment of RE 4*f* (Agui *et al.*, 2004, 2007). Further, the results of our present magnetic Compton scattering measurement of $Tb_{33}Co_{67}$ show that the spin component follows the macroscopic magnetic properties.

We should briefly mention that the MCP effect seems to increase where $H > 0.44$ T. It is expected that the spin component has paramagnetic character. In addition, Takanod *et al.* (2004) reported that magnetization saturation is not achieved on a Fe/Tb multilayer in which the Tb 4*f* and Fe 3*d* components are in opposite magnetic directions. Competition between the Zeeman energy and the exchange energy results in a change of the magnetization in a high magnetic field. However, we did not gain clear evidence of this in the present results; further experiments are needed. We will report on a detailed SSMH study of RE-TM film elsewhere.

4. Conclusion

In this paper, we presented a new application of magnetic Compton scattering measurement for SSMH measurement, and demonstrated its validity. The observed SSMH loop is qualitatively in agreement with the macroscopic *M–H* curve. This new technique has sufficient sensitivity to investigate spin magnetization, even of a thin film. We expect this technique will be adopted as a reliable tool for studying magnetic materials.

This work was performed under the approval of the High Energy Accelerator Research Organization (KEK) and Photon Factory (PF) Advisory Committee (proposal No. 2007G206). The authors would like to thank Drs K. Matsumoto and T. Morikawa for their preparation of samples. We also deeply appreciate useful comments by Drs N. Sakai and M. Mizumaki in discussions with them.

References

Agui, A., Mizumaki, M., Asahi, T., Matsumoto, K., Morikawa, T., Sayama, J. & Osaka, T. (2007). *J. Phys. Chem. Solids*, **68**, 2148–2152.

Agui, A., Mizumaki, M., Asahi, T., Sayama, J., Matsumoto, K., Morikawa, T., Nakatani, T., Matsushita, T., Osaka, T. & Miura, Y. (2004). *Trans. Magn. Soc. Jpn*, **4**, 326–329.

Biggs, F., Mendelsohn, L. B. & Mann, J. B. (1975). *Atom. Data Nucl. Data Tables*, **16**, 201.

Chen, C. T., Idzerda, Y. U., Lin, H.-J., Meigs, G., Chaiken, A., Prinz, G. A. & Ho, G. H. (1993). *Phys. Rev. B*, **48**, R642–R645.

Coey, J. M. D. (1978). *J. Appl. Phys.* **49**, 1646–1652.

Cooper, M. J., Mijnarends, P. E., Shitotani, N., Sakai, N. & Bansil, A. (2004). Editors. *X-ray Compton Scattering.* New York: Oxford University Press.

Kakutani, Y., Kubo, Y., Koizumi, A., Sakai, N., Ahuja, B. L. & Sharma, B. K. (2003). *J. Phys. Soc. Jpn*, **72**, 599–606.

Kawata, H., Miyahara, T., Yamamoto, S., Shioya, T., Kitamura, H., Sato, S., Asaoka, S., Kanaya, N., Iida, A., Mikuni, A., Sato, M., Iwazumi, T., Kitajima, Y. & Ando, M. (1989). *Rev. Sci. Instrum.* **60**, 1885–1888.

Liu, X., Morisako, A., Sakurai, H., Sakurai, Y., Itou, M. & Koizumi, A. (2007). *J. Magn. Magn. Matter.* **310**, 1744–1746.

Sakai, N. (1996). *J. Appl. Cryst.* **29**, 81–99.

Sakai, N., Ito, M., Kawata, H., Iwazumi, T., Ando, M., Shiota, N., Itoh, F., Sakurai, Y. & Nanao, S. (1991). *Nucl. Instrum. Methods Phys. Res. A*, **303**, 488–494.

Sakai, N. & Oono, N. (1976). *Phys. Rev. Lett.* **37**, 351–353.

Sakurai, H., Ota, M., Liu, X., Morisako, A., Sakurai, Y., Itou, M., Nagao, T. & Koizumi, A. (2007). *J. Appl. Phys.* **102**, 013902.

Takanod, K., Ikeuchi, K., Sakurai, H., Oike, H. & Itoh, F. (2004). *J. Phys. Chem. Solids*, **65**, 1985–1992.